



PAPER

Three-dimensional printing of Hela cells for cervical tumor model *in vitro*

To cite this article: Yu Zhao *et al* 2014 *Biofabrication* **6** 035001

View the [article online](#) for updates and enhancements.

You may also like

- [3D bioprinted tumor model with extracellular matrix enhanced bioinks for nanoparticle evaluation](#)
You Chen, Langtao Xu, Weilin Li et al.
- [Ultrasonication-assisted one-step self-assembly preparation of biocompatible fluorescent-magnetic nanobeads for rare cancer cell detection](#)
Shan Guo, Yu-Qi Chen, Ning-Ning Lu et al.
- [Bioprinting of patient-derived *in vitro* intrahepatic cholangiocarcinoma tumor model: establishment, evaluation and anti-cancer drug testing](#)
Shuangshuang Mao, Jianyu He, Yu Zhao et al.

Three-dimensional printing of Hela cells for cervical tumor model *in vitro*

Yu Zhao^{1,2,6}, Rui Yao^{1,2,6}, Liliang Ouyang^{1,2}, Hongxu Ding^{1,2},
Ting Zhang^{1,2}, Kaitai Zhang³, Shujun Cheng³ and Wei Sun^{1,2,4,5,7}

¹ Department of Mechanical Engineering, Biomanufacturing Center, Tsinghua University, Beijing, People's Republic of China

² Biomanufacturing and Rapid Forming Technology Key Laboratory of Beijing, Beijing, People's Republic of China

³ State Key Laboratory of Molecular Oncology, Beijing Key Laboratory for Carcinogenesis and Cancer Prevention, Cancer Institute (Hospital), Peking Union Medical College and Chinese Academy of Medical Sciences, Beijing, People's Republic of China

⁴ Biomanufacturing Engineering Laboratory, Shenzhen Tsinghua Graduate School, Shenzhen, People's Republic of China

⁵ Department of Mechanical Engineering, Drexel University, Philadelphia, PA, USA

E-mail: weisun@tsinghua.edu.cn and sunwei@drexel.edu

Received 31 January 2014, revised 22 February 2014

Accepted for publication 10 March 2014

Published 11 April 2014

Abstract

Advances in three-dimensional (3D) printing have enabled the direct assembly of cells and extracellular matrix materials to form *in vitro* cellular models for 3D biology, the study of disease pathogenesis and new drug discovery. In this study, we report a method of 3D printing for Hela cells and gelatin/alginate/fibrinogen hydrogels to construct *in vitro* cervical tumor models. Cell proliferation, matrix metalloproteinase (MMP) protein expression and chemoresistance were measured in the printed 3D cervical tumor models and compared with conventional 2D planar culture models. Over 90% cell viability was observed using the defined printing process. Comparisons of 3D and 2D results revealed that Hela cells showed a higher proliferation rate in the printed 3D environment and tended to form cellular spheroids, but formed monolayer cell sheets in 2D culture. Hela cells in 3D printed models also showed higher MMP protein expression and higher chemoresistance than those in 2D culture. These new biological characteristics from the printed 3D tumor models *in vitro* as well as the novel 3D cell printing technology may help the evolution of 3D cancer study.

Keywords: 3D cell printing, bioprinting, tumor models, *in vitro* tumor model, cancer model

(Some figures may appear in colour only in the online journal)

1. Introduction

Cancer is one of the most serious diseases, with over 10 million new cases diagnosed worldwide each year. Despite many efforts, an inadequate understanding of tumorigenesis still hinders the development of cancer therapy [1]. Although the most effective way of studying tumors and testing anti-tumor drugs is in clinical trials, ethical and safety limitations

prevent this method from being widely used. To overcome this hurdle, preclinical tumor models are often used to mimic physiological environments of tumors for tumorigenesis study and anti-cancer drug screening [2–4]. For example, Jordan *et al* used two-dimensional (2D) monolayered Hela cell cultures to study the chemotherapy mechanism of the anti-tumor drug paclitaxel (also known as Taxol) [3]. Ellingsen *et al* used surgical specimen xenograft models (animal models) to mimic the physiological microenvironment of cervical carcinoma and studied the mechanism of tumor metastasis and radiation sensitivity [4]. However, 2D monolayered cellular models

⁶ These authors contributed to this work equally.

⁷ Author to whom any correspondence should be addressed.

lack the microenvironment characteristics of natural three-dimensional (3D) tissues *in vivo* [5]. On the other hand, animal models established in immunocompromised mice may show false effects on tumor development and progression [1]. To overcome these hurdles, *in vitro* 3D tumor models based on human cancer cells have been increasingly used in order to accurately reproduce the characteristics of human cancer tissues [6, 7]. Relevant studies of biological characteristics for cell proliferation [8], morphology [9], drug metabolism [10], gene expression and protein synthesis [11] were reported for 3D tumor models which compared with 2D planar culture. Various techniques, such as multicellular spheroids [12–14], cell-seeding 3D scaffolds [11, 15], hydrogel embedding [16, 17], microfluidic chips [18, 19] and cell patterning [20, 21] have also been developed for construction of 3D *in vitro* tumor models. For example, Ridky *et al* reported that the gene alterations in spontaneous tumors were similar to the 3D organotypic tissues in the constructed 3D organotypic tissues seeded with epithelial cells onto basement membranes comparing with the 2D planar cell culture [11]. Loessner *et al* discovered that ovarian cancer cell lines showed higher chemoresistance in 3D hydrogels than in 2D culture [16]. Liu *et al* engineered a microfluidic 3D co-culture tumor model of cancer cells and carcinoma-associated fibroblasts and found increased cancer cell invasion in the 3D microfluidic channels with fibroblast co-culture [19]. Xu *et al* patterned ovarian carcinoma cells and human diploid fibroblast cells onto a 2D Matrigel surface and demonstrated the formation of 3D cellular acini [21]. Although these studies revealed useful characteristics of 3D tumor models *in vitro*, to our knowledge, it is still difficult to simulate a complex 3D physiological tumor microenvironment in most of the above models due to the limitations of the fabrication techniques.

Advances in 3D printing have enabled direct assembly of cells and extracellular matrix (ECM) materials to form *in vitro* cellular models for 3D biology, the study of disease pathogenesis and new drug discovery. This promising technique has offered an opportunity for the biofabrication of complex 3D *in vitro* models with simulated physiological microenvironments [22]. The application of 3D cell printing has been reported in the printing of 3D large-scale tissue constructs [23], *in vitro* liver tissues [24], adipose tissues [25], bone tissues [26] and hybrid tissue constructs with vascular-like networks [27]. The objective of this paper is to report our study on the construction and characterization of *in vitro* cervical tumor models by 3D printing of HeLa cells (cervical tumor cells) and gelatin/alginate/fibrinogen hydrogel biomaterials. Since the HeLa cell line derived from cervical cancer cells was among the first cell lines successfully cultured *in vitro* and was widely used for tumor studies [28], we chose to use HeLa cells for this study. In addition, since native ECM consists of fibrous proteins such as fibronectin, collagen and laminin [29], hydrogels such as alginate [30], fibrin [31] and gelatin [32] are widely used as ECM mimics for cell/tumor cell culture. For this reason we used these materials in this study to print 3D tumor constructs in order to mimic the ECM characteristics and cervical cancer microenvironment. The printing technique and the method of construction of the

3D tumor models will be introduced. The results of biological characterization of cell proliferation, matrix metalloproteinase (MMP) protein expression and chemoresistance for the printed 3D cervical tumor models will be presented and also compared with conventional 2D planar culture models.

2. Materials and methods

2.1. Cell culture

The HeLa cells were obtained from the Center for Animal Experiments/A3 Lab in Wuhan University. The cells were cultured in high-glucose Dulbecco's modified Eagle medium (H-DMEM; Invitrogen) with 10% fetal bovine serum (FBS; Hyclone) in a CO₂ incubator at 37 °C and with 5% CO₂. The HeLa cells were subcultured by trypsin (0.25%; invitrogen) dissociation at about 80% confluence. The culture media were changed every 2–3 days.

2.2. Material preparation

Gelatin powder (Sigma; G1890) was dissolved in 0.9% NaCl solution (w/v) at 20% (w/v). Sodium alginate powder (Sigma; A0682) was dissolved in 0.9% NaCl solution (w/v) at 4% (w/v). Both solutions were sterilized by heating three times in a stove (70 °C) for 30 min. Fibrinogen (Sigma; F8630) was dissolved in H-DMEM at 8% (w/v).

2.3. Construct fabrication and culture

A 3D cell printer developed by our group (cell assembly system I) was used to fabricate 3D tumor-like constructs similar to those previously described [23, 27]. Briefly, HeLa cells were collected by centrifuge at 1000 r min⁻¹ for 5 min and suspended in an 8% fibrinogen solution to a density of 4 × 10⁶ cells mL⁻¹. A fibrinogen/HeLa mixture, 20% gelatin solution and 4% sodium alginate solution were evenly mixed at a volume ratio of 1:2:1. Finally, the mixture was composed of 10% gelatin, 1% sodium alginate, 2% fibrinogen and HeLa cells with a density of 10⁶ cells mL⁻¹. One milliliter of the cell/biomaterial mixture was drawn into a sterilized commercial syringe with a 25 gauge needle. The mixture was physically crosslinked at 25 °C for about 5 min in the syringe and then mounted onto the 3D cell printer. A HeLa/hydrogel construct with a grid structure of 10 × 10 × 2 mm³ was fabricated by forced extrusion in a sterile atmosphere of 10 °C in a layer-by-layer fashion. CaCl₂ (3%, w/v) was gently added to chemically crosslinked alginate in the 3D constructs. The construct was then immersed in 20 U mL⁻¹ thrombin (Sigma; T4648) for 15 min to crosslink fibrinogen. Between each solution addition, the constructs were gently washed in phosphate buffered saline (PBS) two to three times (figure 1(A)). Each construct was cultured in a 35 mm petri dish with 2 mL culture media per dish.

A 2D planar culture sample was prepared by seeding HeLa at a density of 5000 cells cm⁻² in 35 mm petri dishes with 2 mL culture media per dish. Both 3D HeLa/hydrogel constructs and 2D samples were cultured in H-DMEM supplemented with 20 mg L⁻¹ aprotinin (YEASEN) and 10% FBS at 37 °C

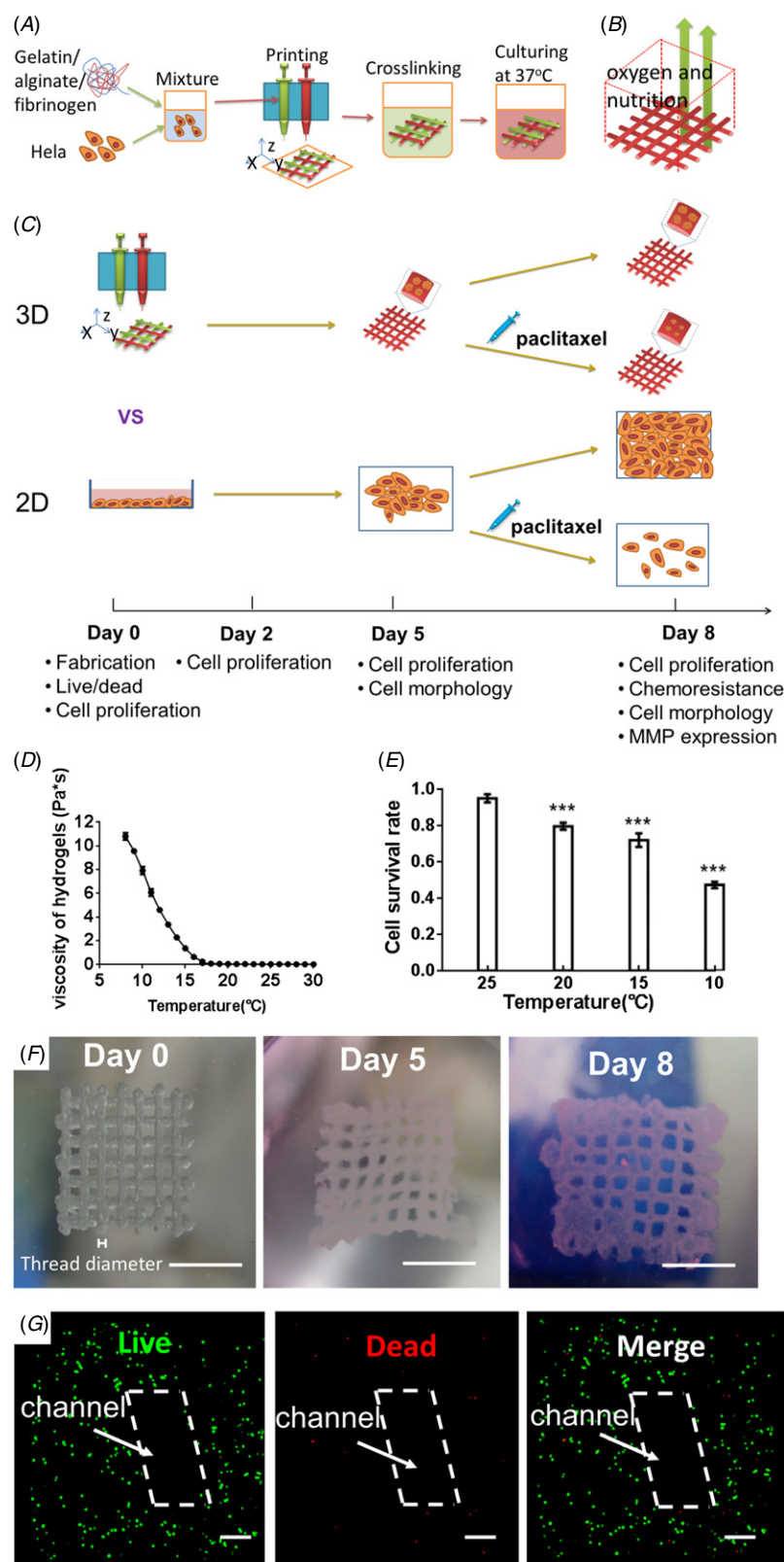


Figure 1. Fabrication of 3D HeLa/hydrogel constructs. (A) Schematic of the 3D cell printing process. (B) The design of the 3D HeLa/hydrogel constructs. (C) Schematic of the timeline of this research. Both 3D HeLa/hydrogel constructs and 2D planar samples were cultured for 5 days and 3 more days with/without paclitaxel addition. (D) The viscosity of hydrogels at different temperatures. (E) Cell survival rate at different temperatures. *** means $p < 0.001$; t -test. (F) Top view of 3D HeLa/hydrogel constructs on day 0, day 5 and day 8. Scale bar, 5 mm. (G) Cell viability after printing by live/dead staining under LSCM, where live cells are stained in green and dead cells are stained in red. Scale bar, 200 μm.

with 5% CO₂ for 8 days. Aprotinin, a proteinase inhibitor, was dissolved in the culture medium to inhibit the fibrin degradation and keep the constructs stable [33]. The culture media were changed on day 2 and 5. The culture medium was collected and centrifuged at 1000 r min⁻¹ for 5 min for MMP expression tests on day 8. The timeline of this research is shown in figure 1(B).

2.4. Viscosity of *Hela*/hydrogels

Before crosslinking (as described in section 2.3) the *Hela*/hydrogel mixture was added into the rotational rheometer (MCR302, Anton Paar) to analyze the viscosity. The shear rate was constant (100 s⁻¹) and the temperature changed from 30 °C to 8 °C. Then the viscosity was recorded every 5 s. Three independent samples were tested.

2.5. Cell survival rate

Three independent samples were printed at different nozzle temperatures. Cell survival rate in the 3D *Hela*/hydrogel constructs was assessed immediately after biofabrication to determine the influence of the printing process on cell viability. A fluorescent live/dead staining was carried out according to the manufacturer's instructions. Briefly, the mixture of Calcein-AM (Dojindo; 1 μmol mL⁻¹) and PI (Sigma; 2 μmol mL⁻¹) was filtered through a 0.22 μm filter prior to staining. *Hela*/hydrogel constructs were stained by incubation with a Calcein AM-PI mixture for 30 min in the dark at 37 °C and gently washed three times with PBS. A laser scanning confocal microscope (LSCM; LSM710META, ZEISS) was used for image acquisition. Cell viability was calculated as (number of green stained cells/number of total cells) × 100%. Three random fields were chosen for each sample. Three independent samples were counted.

2.6. Cell proliferation analysis

The cell counting kit-8 (CCK-8; Dojindo) was used to analyze cell proliferation of both 3D *Hela*/hydrogel constructs and 2D planar culture samples on days 0, 2, 5 and 8 according to the manufacturer's instructions. Briefly, both 3D *Hela*/hydrogel constructs and 2D planar culture samples were washed with PBS three times. Then 1 mL H-DMEM and 0.1 mL CCK-8 solution was added into each 35 mm petri dish. After 2 h of incubation at 37 °C, 0.5 mL culture medium was transferred to a 96-well plate and read by fluorescence with an excitation 450 nm and emission 630 nm filter pair (Model680, Bio-Rad). 3D *Hela*/hydrogel constructs without cells and petri dishes without cells were subjected to the same process to use as blanks. The data of both 3D *Hela*/hydrogel constructs and 2D planar culture samples were normalized to day 0 (4 h after biofabrication or 2D cell seeding). Three independent samples were tested in each group.

2.7. Cell morphology imaging and analysis

A phase-contrast microscope (DP70, Olympus) was used to observe and record cell morphology during the whole

experimental process. Staining of f-actin filaments and cellular nuclei was also applied to determine cellular morphological change in 3D *Hela*/hydrogel constructs and 2D planar culture. Briefly, samples were washed with PBS three times, fixed with 4% paraformaldehyde for 20 min, permeabilized for 30 min by 0.1% Triton X-100, blocked with 1% bovine serum albumin for 30 min and then stained with FITC-phalloidin (5 μg mL⁻¹; Sigma) for 20 min at room temperature with light avoidance. Cell nuclei were stained with DAPI (1 μg mL⁻¹; Sigma) for 5 min at room temperature with light avoidance. Samples were washed with PBS three times between incubations. LSCM (LSM710META, ZEISS) was used for image acquisition.

To quantify morphological changes of *Hela* in the 3D model, phase-contrast microscope images were quantitatively analyzed by Image Pro Plus software. Three images at three different positions were measured. LSCM images were quantitatively analyzed using ZEN 2009 software. Four different positions with more than ten cellular spheroids in each position were measured.

2.8. Protein characterization

The collected supernatant for MMP expression described in section 2.3 was mixed with loading buffer and loaded onto 12% acrylamide gel containing gelatin. Protein concentrations were determined using a BCA kit (Pierce, Rockford, IL) for normalizing the protein amount of 3D *Hela*/hydrogel constructs and 2D planar culture samples. Gel was run at 110 V for 100 min (Electrophoresis System, Bio-Rad) and then treated by an MMP Zymography Assay Kit (Applygen) according to the standard protocol. Gel was then stained in Coomassie brilliant blue staining buffer for 3 h, de-stained until clear bands were visible and semi-quantified by Quantity One software. Three independent samples were tested in each group.

2.9. Chemoresistance test

As shown in figure 1(B), three independent 2D and 3D samples were randomly picked out on day 5 for chemoresistance studies. Briefly, samples were cultured in H-DMEM supplemented with 20 mg L⁻¹ aprotinin, 10% FBS and 50 μg L⁻¹ paclitaxel (Gene Operation) for another 3 days, and tested using a CCK-8 kit as described in section 2.5.

2.10. Statistical analysis

Statistical analysis was performed by GraphPad Prism using two-way analysis of variance (ANOVA) in conjugation with a Bonferroni post-hoc test and a Student t-test. Differences were considered statistically significant when p values were lower than 0.05. All data are presented as mean ± standard deviation. Three independent trials were carried out unless otherwise stated.

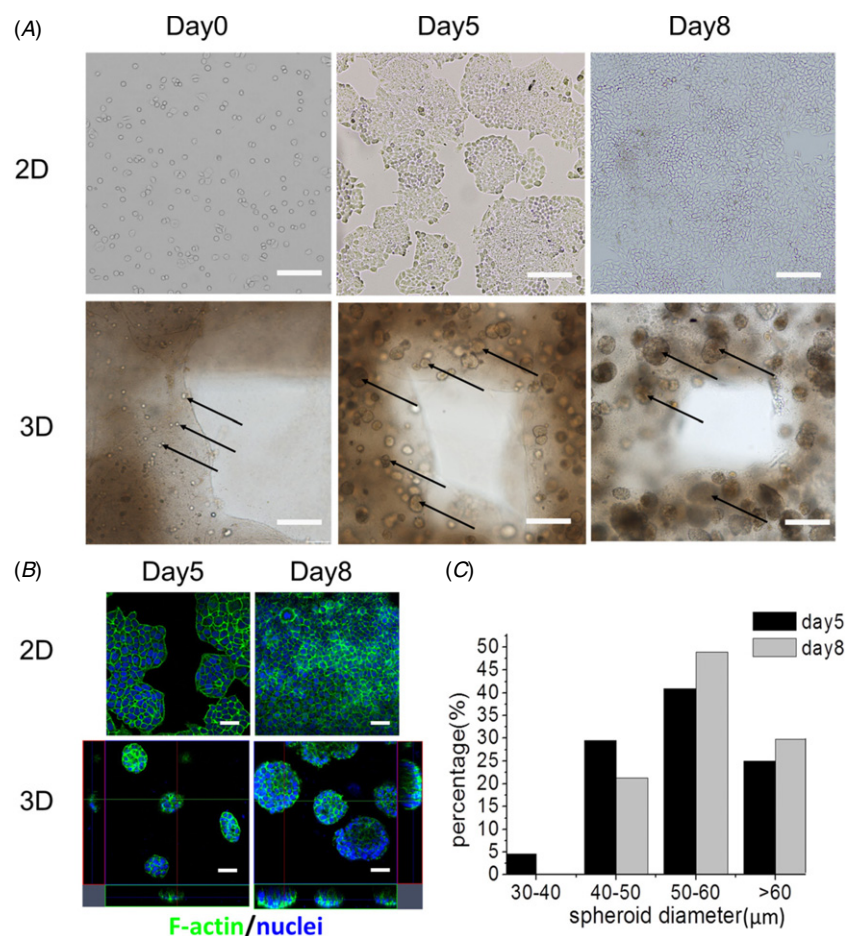


Figure 2. Cellular morphological changes during 8 days of culture in 3D constructs and 2D planar culture. (A) HeLa cells in 2D planar culture and 3D HeLa/hydrogel constructs observed by a phase-contrast microscope on day 0, day 5 and day 8. Scale bar, 200 μm . Black arrows indicate cells and cellular spheroids in the 3D construct. (B) Cytoskeleton distribution by staining on day 5 and day 8 in 2D planar culture and 3D constructs observed under LSCM. Scale bar, 50 μm . (C) Distribution of spheroid diameter in 3D HeLa/hydrogel constructs on day 5 and day 8.

3. Results

3.1. Fabrication of 3D tumor-like constructs

In order to construct 3D tumor models *in vitro* to mimic natural cervical tumors, we used cell printing technology to fabricate 3D HeLa/gelatin/alginate/fibrinogen constructs. A cuboid structure with interconnected channels (figure 1(C)) was designed to allow the transport of nutrients, oxygen and metabolic waste. As shown in figure 1(D), the viscosity of HeLa/hydrogel increased with the decline of hydrogel temperature (30 $^{\circ}\text{C}$ to 10 $^{\circ}\text{C}$), and the viscosity of HeLa/hydrogel increased significantly at the temperature range from 20 $^{\circ}\text{C}$ to 10 $^{\circ}\text{C}$. The cell survival rate decreased with the decline of the nozzle temperature from 25 $^{\circ}\text{C}$ to 10 $^{\circ}\text{C}$, with significant differences (figure 1(E)). We chose the parameters of 10 $\text{mm}^3 \text{min}^{-1}$ extrusion speed, 250 μm nozzle inner diameter, 10 $^{\circ}\text{C}$ chamber temperature and 25 $^{\circ}\text{C}$ nozzle temperature to print 3D HeLa/hydrogel constructs. The printed 3D HeLa/hydrogel constructs showed a clear and stable structure with interconnected channels. The fibers of 3D HeLa/hydrogel constructs were uniform and smooth with a mean thread diameter of 500 μm (figure 1(F)). HeLa/hydrogel

constructs maintained good structural stability for 8 days (figure 1(F)). After printing, the viability of HeLa cells in the constructs was $94.9\% \pm 2.2\%$ (figure 1(G)).

3.2. Cellular morphological change in 3D constructs and 2D culture

A phase-contrast microscope was used to observe the morphology of HeLa cells over an 8 day experimental period in the tumor-like constructs, as shown in figure 2(A). Compared with 2D planar culture, HeLa cells in 3D HeLa/hydrogel constructs showed a spheroid morphology on day 5, and their diameters continued to grow until day 8. Based on semi-quantitative analysis of phase-contrast microscope images, $79.5\% \pm 6.8\%$ areas of hydrogel were taken up by HeLa spheroids. To further analyze cellular morphology in the 3D constructs, cell filaments and nuclei were visualized by staining and observed under LSCM, as shown in figure 2(B). It was demonstrated that HeLa cells formed round spheroids with smooth surfaces and tight cell-cell connections within the 3D hydrogel, whereas HeLa cells cultured on 2D tissue culture plates showed a flat and elongated morphology. Image-based semi-quantitative analysis showed increased spheroid

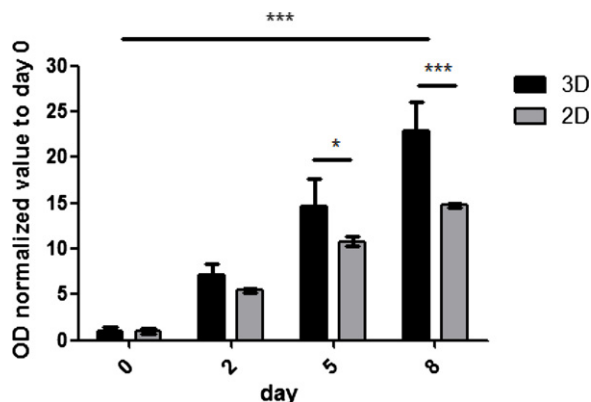


Figure 3. Cellular metabolic change in 2D planar culture and 3D constructs from day 0 to day 8. * means $p < 0.05$, *** means $p < 0.001$; ANOVA in conjunction with Bonferroni *post-hoc* test.

diameter from day 5 ($44 \mu\text{m} \pm 7 \mu\text{m}$) to 8 ($58 \mu\text{m} \pm 10 \mu\text{m}$) (figure 2(C)).

3.3. Cell proliferation and MMP expression

To determine cell proliferation in 3D tumor-like constructs and 2D culture, a CCK-8 kit was used to analyze cellular metabolic activity on day 0, 2, 5 and 8. 2D samples were treated under the same protocol as 3D constructs. It was demonstrated that, compared with day 0, HeLa cells in the 2D planar culture showed 5.4-fold proliferation on day 2, 10.8-fold proliferation on day 5 and 14.8-fold proliferation on day 8, while HeLa cells in 3D HeLa/hydrogel constructs showed 7.2-fold proliferation on day 2, 14.6-fold proliferation on day 5 and 22.8-fold proliferation on day 8. There were significant differences between 3D and 2D samples on day 5 and 8 (figure 3).

MMP-2 and MMP-9 secretion was analyzed using an MMP Zymography assay kit to determine whether the 3D hydrogel environment affected HeLa MMP secretion. As shown in figure 4(A), the bands of both MMP-2 and MMP-9 in 3D HeLa/hydrogel constructs were brighter compared with those in the 2D planar culture. Semi-quantitative grayscale analysis of the bands further indicated that MMP-9 and MMP-2 secretion in 3D construct was 2.3 times and 2.5 times that of the 2D sample, with significant differences (figure 4(B)).

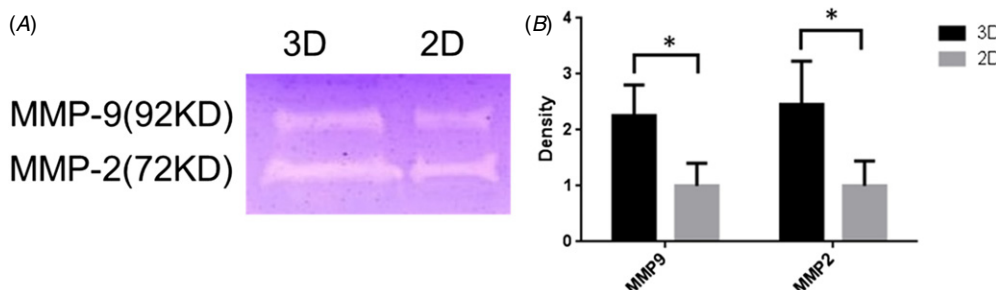


Figure 4. MMP secretion of HeLa cells in 3D constructs and 2D planar culture. (A) MMP-9 and MMP-2 secretion of HeLa cells in 3D constructs and 2D planar culture. (B) Semi-quantitative analysis of MMP-2 and MMP-9 secretion in 3D construct normalized to 2D samples. * means $p < 0.05$; *t*-test.

3.4. Chemoresistance

Paclitaxel was added into the culture media of the 3D tumor-like constructs and 2D culture samples and incubated for three days to analyze chemoresistance of HeLa cells in different conditions. Abundant cellular apoptosis was observed in both the 2D cell culture and 3D constructs after the addition of paclitaxel. The cell morphology became irregular and the cytoskeleton showed loosened morphology (figure 5(A)). Most cells in the 2D culture floated from the substrate, while cellular spheroids in the 3D HeLa/hydrogel constructs were still maintained within the hydrogel threads.

Figure 5(B) demonstrates a dramatic decline of cellular metabolic activity after the addition of paclitaxel. Compared with day 5, which was when paclitaxel was first added, the metabolic activity declined to 0.74 and 0.09 times in the 3D and 2D samples, respectively, with significant differences. Compared with the positive control, which was cultured in H-DMEM without adding paclitaxel, the paclitaxel-added samples showed 0.47 and 0.06 times the metabolic activity in 3D and 2D culture, respectively, with significant differences.

Semi-quantitative analysis of cellular spheroid diameters (figure 5(C)) showed a largely declined mean diameter and non-uniform distribution in the paclitaxel group ($40 \mu\text{m} \pm 14 \mu\text{m}$) compared with the non-paclitaxel group ($58 \mu\text{m} \pm 10 \mu\text{m}$).

4. Discussion

3D tumor models with microenvironmental characteristics of cell-cell and cell-matrix interactions *in vivo* are becoming important tools for drug testing and tumor biological studies [1, 2, 5]. In this study, we printed 3D HeLa/hydrogel constructs as cervical tumor models, and 3D tumor characteristics were studied.

Cell survival rate is one of the key factors to consider while applying 3D cell printing technology in the construction of tissue-like models. Cells are subjected to mechanical forces during the 3D extrusion cell printing process. It is well known that increased mechanical forces cause cellular damage and thus reduce cell survival rate [34]. Mechanical forces in the 3D cell printing process are determined by parameters like extrusion speed, nozzle diameter, viscosity of hydrogels, chamber temperature and nozzle temperature. Decreasing the nozzle diameter, increasing the extrusion speed and increasing

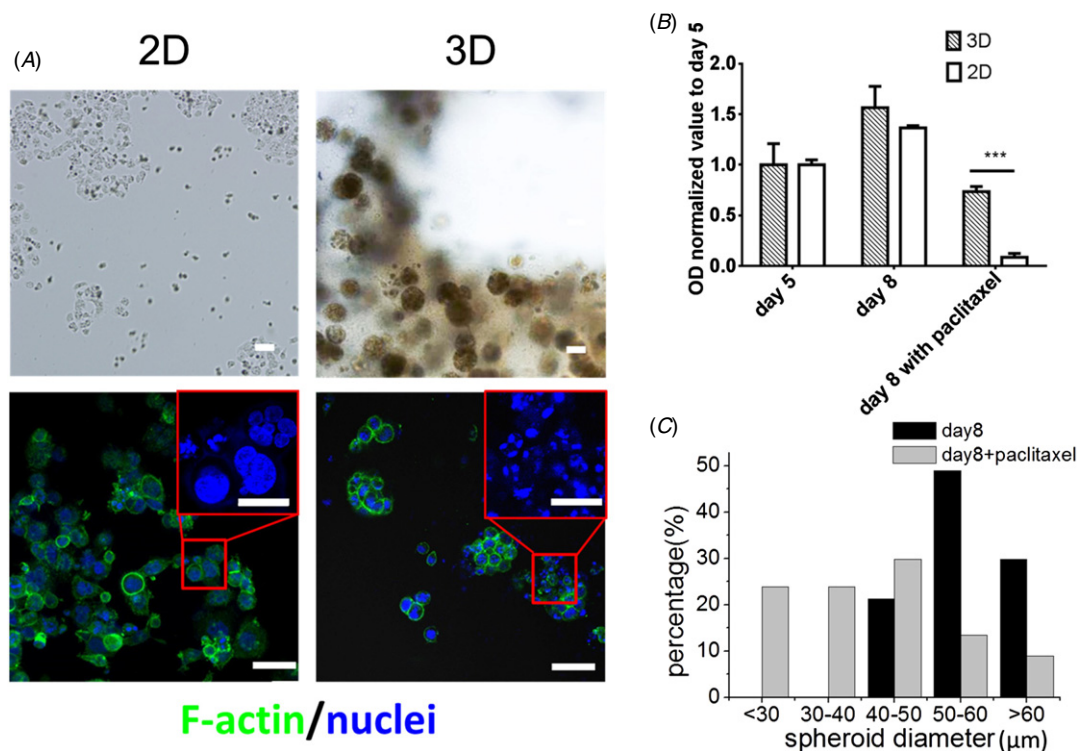


Figure 5. Chemoresistance of HeLa cells in 3D HeLa/hydrogel constructs and 2D planar culture. (A) Cell morphology after paclitaxel treatment in 2D planar culture and 3D HeLa/hydrogel constructs. (B) Cellular metabolic activity after paclitaxel treatment in 2D planar culture and 3D HeLa/hydrogel constructs. (C) Distribution of spheroid diameters in 3D HeLa/hydrogel constructs on day 8 with and without the addition of paclitaxel. *** means $p < 0.001$; t -test. Scale bar, 50 μm (enlarged images, scale bar, 20 μm).

the viscosity of hydrogels results in an increase of shear forces on embedded cells, causing more cellular injury and death. As a thermosensitive hydrogel, the viscosity of gelatin increases with the decline of the hydrogel temperature. As a result, decreasing the chamber or nozzle temperature leads to increased hydrogel viscosity and decreased cellular viability after 3D printing. On the other hand, adequate hydrogel viscosity must be guaranteed to ensure the clear structure and stability of the 3D construct. In this study, we examined the process parameters to achieve both high cellular viability and a stable and clear structure (figures 1(F) and (G)).

Compared with the 2D planar culture, the additional dimensionality of 3D culture leads to differences in cell activities, including morphology, proliferation, and gene and protein expression [35]. We used an optical microscope and observed big differences in HeLa morphology between 3D printed constructs and 2D planar culture. To further investigate this point, cytoskeletons and cell nuclei were treated by staining and observed under LSCM. HeLa cells in 2D culture showed a monolayered morphology in the whole experimental period, whereas cellular spheroids were formed from single cells in 3D tumor-like constructs. Similar observations were reported for studies on epithelial cancer cells in 3D culture [36, 37]. Multicellular tumor spheroids with *in vivo* tumor characteristics of avascular tumor nodules are the classic 3D tumor models *in vitro* for anti-tumor drug testing [38–40]. However, the cellular spheroids established by traditional approaches (e.g. hanging drop [12]) were not embedded within matrix biomaterials. Cells were embedded

within gels to promote cellular spheroid formation along with cell–matrix interactions [41]. Cellular spheroids in 3D gels usually have a polarized property that faces the gel at the basal compartment and encloses at the apical compartment [35], which is more similar to the manner *in vivo* compared with the 2D planar cell culture. The cell morphology in 3D printed HeLa/hydrogel constructs was similar to that in 3D embedding gels [16]. We assumed that this was because we first mixed biomaterials (gelatin, alginate and fibrinogen) with single HeLa cells and then printed the mixture layer by layer so that the cells were embedded within the hydrogels immediately after printing.

Enabling replicative immortality is one of the crucial cancer hallmarks [42], but tumor cell proliferation in 2D plates was inevitably inhibited by the area of the growth surface. Although HeLa cells can form multi-layered growth without contact inhibition, the multi-layered cellular aggregates easily float away from the substrate and cause abundant cell loss. 10^6 mL^{-1} was the commonly used cell density in 3D construct fabrication [43]. When HeLa cells were mixed with biomaterials at this density, 3D cellular spheroids were formed in 3D HeLa/hydrogel constructs and continued growing until day 8 without obvious cell loss. However, when HeLa cells were seeded at a similar density (10^6 cm^{-2}) as a 2D planar culture sample, they achieved 100% confluence in 2 to 3 days, and failed to complete the 8-day experiment. Finally, we chose to reduce the HeLa cell seeding density to 5000 cells/ cm^2 in 2D planar cell culture so as to prevent cell floating before 8 days of culture. This result also indicated an important advantage

of 3D cell/hydrogel constructs in supporting long-term cell proliferation and larger quantity number of cell delivery. We chose an 8 day experimental period in this study because cellular spheroids had occupied most of the area ($79.5\% \pm 6.8\%$) in the matrix by day 8.

A CCK-8 kit was used for cell proliferation analysis. OD values of CCK-8 reagents were determined by the dehydrogenase activities in cells, which is in direct ratio to the number of living cells. In this study, we seeded the same number of cells in 2D plates (5000 cells/dish) and 3D constructs (5000 cells/construct) on day 0. However, OD values determined by a CCK-8 kit showed differences between 2D planar culture samples and 3D Hela/hydrogel constructs. We assumed that this was due to penetration differences of CCK-8 agents and/or cellular metabolic productions between elongated monolayered cells on 2D culture plates and spheroid single cells embedded in 3D hydrogels. The data of both the 3D and 2D samples were therefore normalized to day 0 to eliminate the influence of the proliferation kit. Hela cells in the 2D culture plates proliferated more slowly than in the printed 3D constructs with significant differences on day 5 and 8. We assumed that this was due to enhanced cell–cell interactions in the 3D cellular spheroids and cell–matrix interactions between the Hela and matrix biomaterials, although the detailed mechanisms need to be studied more closely. These results were also consistent with reported studies on 3D cervical tumor spheroid models [8].

The MMP protein family is considered fundamental in the degradation of the ECM [44, 45]. The MMP family, in particular MMP-2 and MMP-9, allow cancer cells to penetrate the ECM and are closely related to cancer metastasis [46]. The activity of MMPs tends to increase with the progression of cervical uterine neoplasms [47]. The study of cervical cancer *in vivo* confirmed a higher expression level of the MMP proteins in cervical tumor tissues compared with normal cervical tissues [48]. The activity of MMP proteins in cervical tumors was always studied *in vitro* based on Hela cells [49, 50]. We examined MMP-2 and MMP-9 expression levels as indicators of tumor metastasis characteristics of Hela cells in 2D and 3D conditions. Hela cells in 3D Hela/hydrogel constructs showed enhanced expression of MMP-2 as well as MMP-9 compared with 2D planar culture, indicating enhanced cellular metastasis in 3D printed constructs. This was similar to the studies on 3D glioma tumor models based on cell-seeding scaffolds [30].

Chemoresistance to anti-cancer drugs represents an important characteristic of enhanced tumor malignancy [51]. Monolayered cell culture with largely enhanced drug agent penetration always failed to mimic *in vivo* tumor characteristics. It has been demonstrated that cellular spheroids showed enhanced resistance to anti-tumor drugs compared with 2D planar cell culture [40, 52, 53]. Paclitaxel is a widely used anti-tumor drug which can mediate cell cycle arrest and cause apoptosis of tumor cells [16]. It is also known to induce a sustained mitotic block at the metaphase/anaphase boundary of Hela cells and inhibit Hela cell proliferation [3]. We observed massive cellular apoptosis both in 3D printed Hela/hydrogel constructs

and 2D cell cultures after treatment with paclitaxel. After quantifying cellular metabolic activity with a CCK-8 kit, largely enhanced chemoresistance was observed in the 3D printed Hela/hydrogel constructs compared with the 2D planar cell culture, with significant differences. This result indicated the importance of dimensionality on the effectiveness of chemotherapy.

5. Conclusions

This paper reported a study of applying a 3D printing technique to construct *in vitro* cervical tumor models with Hela cells and gelatin/alginate/fibrinogen hydrogels. Cell proliferation, MMP protein expression and chemoresistance in the printed 3D cervical tumor models were measured and compared with the conventional 2D planar culture models. The study examined the effect of the printing parameters on cell viability, and a cell viability of over 90% was observed in the Hela cells under the printing process. Comparisons of 3D and 2D results reveal that the Hela cells showed a higher proliferation rate in the printed 3D environment and tended to form cellular spheroids, but formed monolayer cell sheets in the 2D culture. Hela cells in 3D printed models also showed higher MMP protein expression and higher chemoresistance than those in 2D culture. The results also reveal that the printed 3D models have more simulated tumor characteristics compared with the 2D planar cell culture models. Those 3D biological characteristics from the printed tumor models *in vitro* as well as the novel 3D cell printing technology may help the study of 3D tumor biology. In addition, the developed 3D printing process is capable of assembling cells with different phenotypes, thus allowing the construction of 3D *in vitro* models with heterogeneous cells to simulate the heterogeneous tumor microenvironment [54]. Therefore, the reported cell printing process may also have a broad application in the study of tumor heterogeneity [54].

Acknowledgments

The authors acknowledge the funding support of the National High Technology Research and Development Program of China (863) through project no 2012AA020506 and the Chinese National Natural Science Foundation through project no 51235006. WS also acknowledges the funding support, in part, from the National Science Foundation through grant no NSF-CMMI-1030520. The authors also acknowledge the valuable comments and time spent by referees to improve this manuscript.

References

- [1] Vargo-Gogola T and Rosen J M 2007 Modelling breast cancer: one size does not fit all *Nature Rev. Cancer* **7** 659–72
- [2] Kim J B 2005 Three-dimensional tissue culture models in cancer biology *Semin. Cancer Biol.* **15** 365–77
- [3] Jordan M A, Toso R J, Thrower D and Wilson L 1993 Mechanism of mitotic block and inhibition of cell proliferation by taxol at low concentrations *Proc. Natl Acad. Sci. USA* **90** 9552–6

- [4] Ellingsen C, Natvig I, Gaustad J-V, Gulliksrud K, Egeland T A and Rofstad E K 2009 Human cervical carcinoma xenograft models for studies of the physiological microenvironment of tumors *J. Cancer Res. Clin. Oncol.* **135** 1177–84
- [5] Padrón J M, van der Wilt C L, Smid K, Smitskamp-Wilms E, Backus H H, Pizao P E, Giaccone G and Peters G J 2000 The multilayered postconfluent cell culture as a model for drug screening *Crit. Rev. Oncol. Hematol.* **36** 141–57
- [6] Bissell M J and Radisky D 2001 Putting tumours in context *Nature Rev. Cancer* **1** 46–54
- [7] Horning J L, Sahoo S K, Vijayaraghavalu S, Dimitrijevic S, Vasir J K, Jain T K, Panda A K and Labhasetwar V 2008 3D tumor model for *in vitro* evaluation of anticancer drugs *Mol. Pharm.* **5** 849–62
- [8] Chopra V, Dinh T and Hannigan E 1997 Three-dimensional endothelial-tumor epithelial cell interactions in human cervical cancers *In Vitro Cell. Dev. Biol. Anim.* **33** 432–42
- [9] Li C L, Tian T, Nan K J, Zhao N, Guo Y H, Cui J, Wang J and Zhang W G 2008 Survival advantages of multicellular spheroids versus monolayers of HepG2 cells *in vitro Oncol. Rep.* **20** 1465–71
- [10] Loessner D, Rizzi S C, Stok K S, Fuehrmann T, Hollier B, Magdolen V, Huttmacher D W and Clements J A 2013 A bioengineered 3D ovarian cancer model for the assessment of peptidase-mediated enhancement of spheroid growth and intraperitoneal spread *Biomaterials* **34** 7389–400
- [11] Ridky T W, Chow J M, Wong D J and Khavari P A 2010 Invasive three-dimensional organotypic neoplasia from multiple normal human epithelia *Nature Med.* **16** 1450–5
- [12] Del Duca D, Werbowetski T and Del Maestro R F 2004 Spheroid preparation from hanging drops: characterization of a model of brain tumor invasion *J. NeuroOncol.* **67** 295–303
- [13] Kelm J M, Timmins N E, Brown C J, Fussenegger M and Nielsen L K 2003 Method for generation of homogeneous multicellular tumor spheroids applicable to a wide variety of cell types *Biotechnol. Bioeng.* **83** 173–80
- [14] Ma H L, Jiang Q, Han S, Wu Y, Tomshine J C, Wang D, Gan Y, Zou G and Liang X J 2012 Multicellular tumor spheroids as an *in vivo*-like tumor model for three-dimensional imaging of chemotherapeutic and nano material cellular penetration *Mol. Imaging* **11** 487–98 (PMID: 23084249)
- [15] Fischbach C, Chen R, Matsumoto T, Schmelzle T, Brugge J S, Pulverini P J and Mooney D J 2007 Engineering tumors with 3D scaffolds *Nature Methods* **4** 855–60
- [16] Loessner D, Stok K S, Lutolf M P, Huttmacher D W, Clements J A and Rizzi S C 2010 Bioengineered 3D platform to explore cell–ECM interactions and drug resistance of epithelial ovarian cancer cells *Biomaterials* **31** 8494–506
- [17] Szot C S, Buchanan C F, Freeman J W and Rylander M N 2011 3D *in vitro* bioengineered tumors based on collagen: I. Hydrogels *Biomaterials* **32** 7905–12
- [18] Hsiao A Y, Torisawa Y-S, Tung Y-C, Sud S, Taichman R S, Pienta K J and Takayama S 2009 Microfluidic system for formation of PC-3 prostate cancer co-culture spheroids *Biomaterials* **30** 3020–7
- [19] Liu T, Lin B and Qin J 2010 Carcinoma-associated fibroblasts promoted tumor spheroid invasion on a microfluidic 3D co-culture device *Lab Chip* **10** 1671–7
- [20] Dickinson L E, Lutgebaucks C, Lewis D M and Gerecht S 2012 Patterning microscale extracellular matrices to study endothelial and cancer cell interactions *in vitro Lab Chip* **12** 4244–8
- [21] Xu F, Celli J, Rizvi I, Moon S, Hasan T and Demirci U 2011 A three-dimensional *in vitro* ovarian cancer coculture model using a high-throughput cell patterning platform *Biotechnol. J.* **6** 204–12
- [22] Mironov V, Trusk T, Kasyanov V, Little S, Swaja R and Markwald R 2009 Biofabrication: a 21st century manufacturing paradigm *Biofabrication* **1** 022001
- [23] Yan Y, Wang X, Pan Y, Liu H, Cheng J, Xiong Z, Lin F, Wu R, Zhang R and Lu Q 2005 Fabrication of viable tissue-engineered constructs with 3D cell-assembly technique *Biomaterials* **26** 5864–71
- [24] Chang R, Emami K, Wu H and Sun W 2010 Biofabrication of a three-dimensional liver micro-organ as an *in vitro* drug metabolism model *Biofabrication* **2** 045004
- [25] Yao R, Zhang R J, Yan Y N and Wang X H 2009 *In vitro* angiogenesis of 3D tissue engineered adipose tissue *J. Bioactive Compatible Polym.* **24** 5–24
- [26] Fedorovich N E, De Wijn J R, Verbout A J, Alblas J and Dhert W J 2008 Three-dimensional fiber deposition of cell-laden, viable, patterned constructs for bone tissue printing *Tissue Eng. A* **14** 127–33
- [27] Li S, Xiong Z, Wang X, Yan Y, Liu H and Zhang R 2009 Direct fabrication of a hybrid cell/hydrogel construct by a double-nozzle assembling technology *J. Bioactive Compatible Polym.* **24** 249–65
- [28] Nelson-Rees W A and Flandermeyer R R 1976 HeLa cultures defined *Science* **191** 96–8
- [29] Tibbitt M W and Anseth K S 2009 Hydrogels as extracellular matrix mimics for 3D cell culture *Biotechnol. Bioeng.* **103** 655–63
- [30] Kievit F M, Florczyk S J, Leung M C, Veisheh O, Park J O, Disis M L and Zhang M 2010 Chitosan–alginate 3D scaffolds as a mimic of the glioma tumor microenvironment *Biomaterials* **31** 5903–10
- [31] Clark R A, Lin F, Greiling D, An J and Couchman J R 2004 Fibroblast invasive migration into fibronectin/fibrin gels requires a previously uncharacterized dermatan sulfate-CD44 proteoglycan *J. Invest. Dermatol.* **122** 266–77
- [32] Paguirigan A and Beebe D 2006 Gelatin based microfluidic devices for cell culture *Lab Chip* **6** 407–13
- [33] Ye Q, Zund G, Benedikt P, Jockenhoevel S, Hoerstrup S P, Sakyama S, Hubbell J A and Turina M 2000 Fibrin gel as a three dimensional matrix in cardiovascular tissue engineering *Eur. J. CardioThorac. Surg.* **17** 587–91
- [34] Chang R and Sun W 2008 Effects of dispensing pressure and nozzle diameter on cell survival from solid freeform fabrication-based direct cell writing *Tissue Eng. A* **14** 41–8
- [35] Schwartz M A and Chen C S 2013 Deconstructing dimensionality *Science* **339** 402–4
- [36] Weaver V M, Petersen O W, Wang F, Larabell C, Briand P, Damsky C and Bissell M J 1997 Reversion of the malignant phenotype of human breast cells in three-dimensional culture and *in vivo* by integrin blocking antibodies *J. Cell Biol.* **137** 231–45
- [37] Lee G Y, Kenny P A, Lee E H and Bissell M J 2007 Three-dimensional culture models of normal and malignant breast epithelial cells *Nature Methods* **4** 359–65
- [38] Hamilton G 1998 Multicellular spheroids as an *in vitro* tumor model *Cancer Lett.* **131** 29–34
- [39] Kunz-Schughart L A, Kreutz M and Knuechel R 1998 Multicellular spheroids: a three-dimensional *in vitro* culture system to study tumour biology *Int. J. Exp. Pathol.* **79** 1–23
- [40] Friedrich J, Ebner R and Kunz-Schughart L A 2007 Experimental anti-tumor therapy in 3-D: spheroids—old hat or new challenge? *Int. J. Radiat. Biol.* **83** 849–71
- [41] Pampaloni F, Reynaud E G and Stelzer E H 2007 The third dimension bridges the gap between cell culture and live tissue *Nature Rev. Mol. Cell Biol.* **8** 839–45
- [42] Hanahan D and Weinberg R A 2011 Hallmarks of cancer: the next generation *Cell* **144** 646–74
- [43] Yao R, Du Y, Zhang R, Lin F and Luan J 2013 A biomimetic physiological model for human adipose tissue by adipocytes

- and endothelial cell cocultures with spatially controlled distribution *Biomed. Mater.* **8** 045005
- [44] Woessner J F 2002 MMPs and TIMPs—an historical perspective *Mol. Biotechnol.* **22** 33–49
- [45] Nagase H and Woessner J F 1999 Matrix metalloproteinases *J. Biol. Chem.* **274** 21491–4
- [46] Brinckerhoff C E and Matrisian L M 2002 Matrix metalloproteinases: a tail of a frog that became a prince *Nature Rev. Mol. Cell Biol.* **3** 207–14
- [47] Libra M, Scalisi A, Vella N, Clementi S, Sorio R, Stivala F, Spandidos D A and Mazzarino C 2009 Uterine cervical carcinoma: role of matrix metalloproteinases (review) *Int. J. Oncol.* **34** 897–903
- [48] Nair S A, Karunakaran D, Nair M and Sudhakaran P 2003 Changes in matrix metalloproteinases and their endogenous inhibitors during tumor progression in the uterine cervix *J. Cancer Res. Clin. Oncol.* **129** 123–31
- [49] Roomi M, Monterrey J, Kalinovsky T, Rath M and Niedzwiecki A 2010 *In vitro* modulation of MMP-2 and MMP-9 in human cervical and ovarian cancer cell lines by cytokines, inducers and inhibitors *Oncol. Rep.* **23** 605–14
- [50] Roomi M, Monterrey J, Kalinovsky T, Rath M and Niedzwiecki A 2009 Patterns of MMP-2 and MMP-9 expression in human cancer cell lines *Oncol. Rep.* **21** 1323
- [51] Jang S H, Wientjes M G, Lu D and Au J L-S 2003 Drug delivery and transport to solid tumors *Pharm. Res.* **20** 1337–50
- [52] Desoize B and Jardillier J-C 2000 Multicellular resistance: a paradigm for clinical resistance? *Crit. Rev. Oncol. Hematol.* **36** 193–207
- [53] Mikhail A S, Eetezadi S and Allen C 2013 Multicellular tumor spheroids for evaluation of cytotoxicity and tumor growth inhibitory effects of nanomedicines *in vitro*: a comparison of docetaxel-loaded block copolymer micelles and taxotere® *PloS One* **8** e62630
- [54] Junttila M R and de Sauvage F J 2013 Influence of tumour micro-environment heterogeneity on therapeutic response *Nature* **501** 346–54